Area Selectivity of InGaAsP–InP Multiquantum-Well Intermixing by Impurity-Free Vacancy Diffusion

Sang Kee Si, Deok Ho Yeo, Kyung Hun Yoon, and Sung June Kim

***Abstract*—Area selectivity of bandgap tuning in the InGaAsP-InP multiquantum-well structure has been investigated using low temperature photoluminescence (PL). The bandgap blue-shift in the intermixed region was as much as 170 meV for a rapid thermal annealer anneal of 30 s at 850 °C, and was controllable using annealing temperature and time. From samples with SiO_2 stripe patterns, clearly separated PL peaks were observed centered at 0.95 and 1.08 eV, each representing signals originating from the dielectric capped and exposed areas, respectively. In samples with stripes intervals less than 6 μm, PL signals did not separate, but formed one broad spectrum due to lateral diffusion. The lateral diffusion was found less than 3.0 μm.**

***Index Terms*—Area selectivity, bandgap tuning, impurity-free vacancy diffusion (IFVD), InGaAsP–InP multiquantum-well (MQW) structures, lateral diffusion coefficient, quantum-well intermixing.**

I. Introduction

THE SPATIAL bandgap tuning in the InGaAsP–InP multiquantum-well (MQW) structure has been studied intensively for years as an important tool for integrating optical devices operating at more than one wavelength [1]. The regrowth technique [2] can be used for this purpose, but is a complicated process and has low yield. Alternatively one of the quantum-well (QW) disordering techniques can be used where compositional disordering occurs between QW and barrier to cause change in bandgap. Included in this category are impurity-induced disordering (IID) [3], [4], ion-implantation enhanced intermixing (IIEI) [5], [6], and impurity-free vacancy diffusion (IFVD) [7], [8]. In IID or IIEI methods, the area-selective tuning is obtained because in areas where impurities are introduced using diffusion (IID) or using ion implantation (IIEI), the bandgap shift is much larger than in the rest. In IFVD, vacancies are injected into the semiconductor in those areas where dielectric capping is deposited and these vacancies then enhance the intermixing process.

Among these techniques, the IFVD method is of particular interest, especially in the waveguide devices, since optical scattering loss introduced by impurities can be avoided. Typically, an IFVD method involves deposition of a dielectric capping material and subsequent thermal annealing [9], [10]. In GaAs–AlGaAs QW materials, SiO_2 is known to induce out-diffusion of Ga during annealing, and to generate vacancies [11]. These Ga vacancies then propagate down to the QW and enhance the intermixing of Ga and Al. Hence, the bandgap becomes larger in the well material by partial disordering of the two material. In the InGaAs(P)–InP QW materials, an IFVD technique involved the use of SiN_x capping where a bandgap tuning of 150 meV was observed [12]. We have reported recently about using SiO_2 capping on the InGaAs–InP QW where we showed a bandgap blue-shift as large as 230 meV [13]. Simultaneous use of InGaAs cap with the SiO_2 capping was proven critically important while other semiconductor cap-dielectric capping combinations did not show significant bandgap tuning at temperatures ranging from 650 °C to 750 °C.

In terms of the area-selectivity, there has been a report where the intermixing was done using photoabsorption-induced disrodering [14] and the area-selectivity was monitored using time resolved photoluminescence (PL) [15]. However, the lateral spatial resolution obtained in this study was 20 μm and considered excessively large for practical application. In this paper, we first report that our method of using the InGaAs cap–SiO_2 capping can be successfully applied to the InGaAsP–InP QW system. We then demonstrate the area-selectivity of this technique using patterned SiO_2 films and show that the spatial resolution obtained using our method is less than 3 μm.

II. Experimental

Fig. 1 shows the cross-sectional view of epitaxial structure used in this experiment. The MQW grown on an n-type (S-doped; 3×10^{18} cm^{-3}) InP substrate consists of 10 pairs of 45-Å undoped $In_{0.6}Ga_{0.4}As_{0.87}P_{0.13}$ wells and 100-Å undoped InP barriers. A 0.54-μm p-type (6.4×10^{17} cm^{-3}) InP clad layer was then grown on which a 0.1-μm p$^+$-type (1.4×10^{19} cm^{-3}) InGaAs cap layer was finally deposited. The whole structure was grown by low-pressure metal–organic chemical vapor deposition (MOCVD) without interruption. Zn and S were used as p-type and n-type dopants, respectively. Unlike in other studies that used similar quantum wells, we used the InGaAs cap layer instead of InP [13]. A 1700-Å-thick SiO_2 layer was then deposited by plasma enhanced chemical vapor deposition (PECVD) at 300 °C and annealing was performed using a rapid thermal annealer (RTA) for 30 s at various anneal temperatures.

For those samples used for the area-selectivity study, the SiO_2 film was then subject to pattering. Stripe patterns were

Manuscript received January 12, 1998; revised April 8, 1998. This work was supported in part by Korea Telecom Switching Technology Research under Grant 970124 and in part by the Institute of Information Technology Assessment under Grant 97-NF-02-14-a-01.

The authors are with the School of Electrical Engineering, Seoul National University, Seoul 151-742, Korea.

Publisher Item Identifier S 1077-260X(98)05855-9.

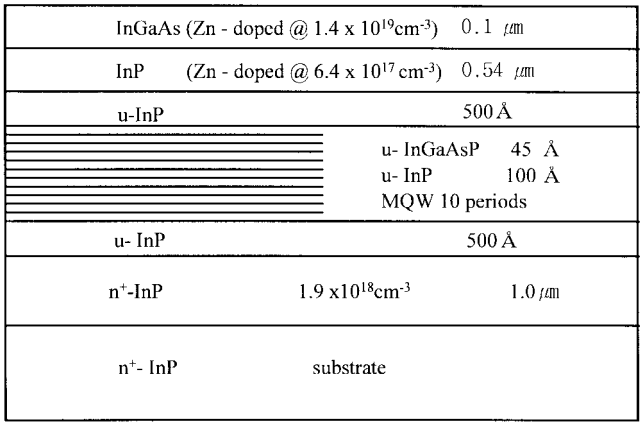

Fig. 1. Schematic cross-sectional view of the MQW structure.

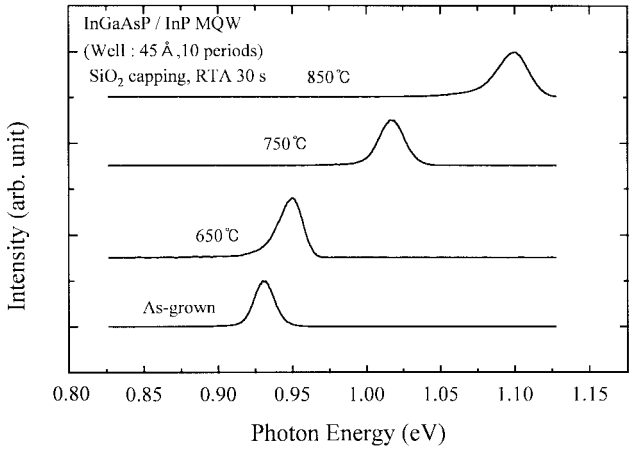

Fig. 2. Normalized PL spectra (at 10 K) obtained from the MQW structure of Fig. 1. The samples were capped with SiO_2 and RTA-annealed for 30 s at temperatures ranging from 650 to 850 °C.

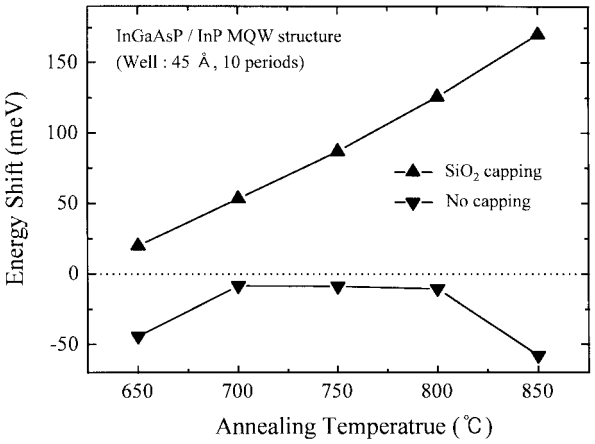

Fig. 3. Amount of shift of PL peak energy plotted as a function of the annealing temperature. The upper trace is for samples with oxide capping while the lower trace is for samples without capping. The annealing time was 30 s.

used where the width of the oxide stripe was set equal to that of the window. Various dimensions ranging from 2 to 50 μm were used for the stripe width. The samples with the stripe SiO_2 patterns were then annealed at 700 °C for 120 s. After annealing, the SiO_2 layer was removed using wet etching. The InGaAs cap layer was also removed by wet etching to improve the PL efficiency at the wavelength range of interest. The shift of the PL peak energy from its as-grown value was used to monitor the degree of the QW intermixing. Low-temperature PL measurements were made at 10 K using a closed cycle He refrigerator. The samples were excited with the 632.8-nm line from He–Ne laser. Luminescence was dispersed using a 0.5-m monochromator at a spectral resolution of 0.5 nm and detected by liquid N_2 cooled Ge detector.

III. Results and Discussion

Fig. 2 shows the normalized PL spectra of the as-grown sample and the samples treated with SiO_2 capping. The dielectric-capped samples were RTA annealed for 30 s at various temperatures. The bandgap energy of as-grown sample was 0.93 eV. In the IFVD treated samples, the bandgap energy increase (blue-shift) was RTA temperature dependent. The energy shifts are 20, 87, and 170 meV for RTA temperature of 650, 750, and 850 °C, respectively. We also noted that the variation of spectral broadening for this temperature range was not large.

We then prepared a sample without the SiO_2 capping and treated it with RTA. The PL spectrum from the sample is shown in Fig. 3 compared with the one taken with the SiO_2 capping. In contrast to the large bandgap blue-shift of the sample with the dielectric capping, the sample without capping showed small red-shifts of the bandgap energy.

The large blue-shift can be explained by strong intermixing caused by the generation of vacancies at the oxide-InGaAs interface. Since interdiffusion can occur for both group-III (In, Ga) and group-V (As, P) in InGaAs(P)–InP QW system [16], the intermixing of InGaAs(P)–InP QW structures is more complicated than in the GaAs–AlGaAs QW material. As in GaAs–AlGaAs QW, we think that the group III vacancies are generated at the InGaAs–SiO_2 interface through the formation of Ga_2O_3. For the group V vacancies, the detailed mechanism of vacancy generation is not known. Assuming that the two types of vacancies are generated at the InGaAs– SiO_2 interface and that they cause interdiffusions in their own sublattices, we can then analyze the intermixing characteristics of our samples. In the analysis, we calculate the postdiffusion energy profiles using two diffusion coefficients for the group-III and group-V interdiffusions and solve Schrödinger's equation to determine the PL peak transition. For the $In_xGa_{1-x}As_yP_{1-y}$ QW we studied, the spatial profile of In and As concentration (x, y) across the well is assumed to have error function distributions [17]. The electron- and heavy-hole subband energies for the interdiffused structures are obtained using finite difference method with an effective mass approximation. The strain effect was also considered [18].

Fig. 4 shows the PL energy shift as a function of diffusion length ($L_d = \sqrt{Dt}$ where D is the diffusion coefficient and t is the anneal time) of the group-III elements. The dotted line shows calculated values at various k ($k = Ld_5/Ld_3$, the ratio of group-V element's diffusion length) to that of group-III element's. The best fitting is obtained using $k =$

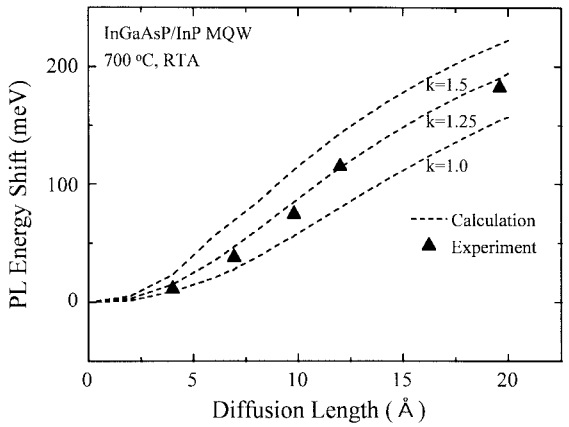

Fig. 4. PL energy shift plotted as a function of diffusion length. The dotted line shows the calculated curve at various k ($k = Ld_5/Ld_3$, the ratio of diffusion length). The x-axis is Ld_3. The solid triangle shows the experimental results.

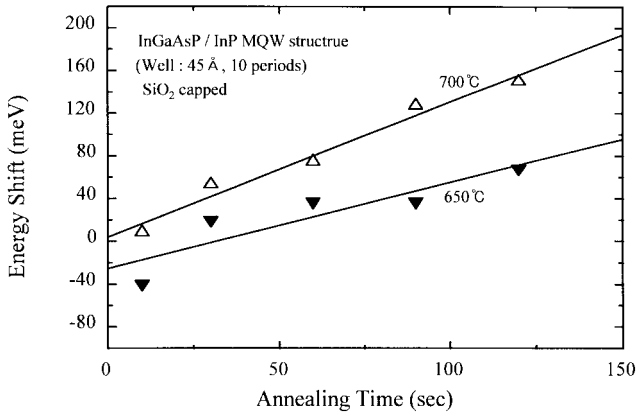

Fig. 5. Amount of shift of PL peak energy plotted as a function of the annealing time for samples capped with SiO_2.

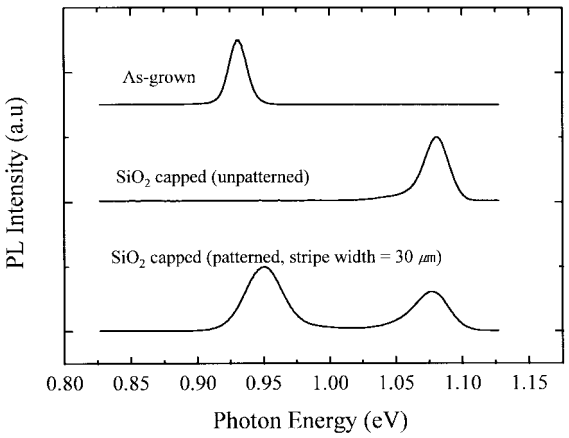

Fig. 6. Normalized PL spectra (at 10 K) for as-grown, oxide-capped, and oxide-patterned MQW structure.

1.25 to the experimental data, that is, the group-V elements has slightly higher diffusion coefficients than the group-III elements. Corresponding diffusion coefficients of group-III and -V interdiffusions are 1.6×10^{-16} cm^{-2}/s, 2×10^{-16} cm^{-2}/s, respectively, at 700 °C.

The slight red-shift observed in the annealed-only samples can be explained using the impurity induced disordering (IID) effect. The Zn doping in the upper clad and cap layers diffuses into the MQW region during the annealing step with the diffusing Zn caused intermixing of group-III elements. Since Zn has fast diffusing species in InP related materials as well as in GaAs, our MQW structure is very likely to have Zn at the diffusion temperatures used. The Zn can then enhance diffusion of group-III elements, causing red shift of PL spectrum. The PL peak observed at 650 °C, however, may be due to the Zn acceptor related emission. The ionization energy of Zn is known to be about 30 meV in the InGaAs material [19]. At higher temperatures, this red-shift is compensated by the blue-shift caused by self-interdiffusion [20], hence the amount of red-shift decreases. However, this does not explain another increase of red-shift occurring at 850 °C, which was a reproducible data. Further study is therefore needed to explain this effect completely. Fig. 5 shows the amount of shift of the bandgap energy calculated from PL spectra when the annealing time was varied from 10–120 s. The maximum amount of blue-shift was 150 meV from a sample annealed at 700 °C for 120 s.

The area-selectivity of the process was then investigated using patterned SiO_2 films as described earlier. Dielectric-patterned samples with windows of 2 to 50 μm width were subject to thermal annealing at 700 °C for 120 s. The He–Ne laser used in the PL had a spotsize of about 500 μm, which was large enough to simultaneously excite multiple number of dielectric-masked and exposed areas. Thus the collected PL signal was the sum of the signals from the two areas.

The PL spectrum shown at the bottom of Fig. 6 is from a pattern where the width of the stripe (and the window) was 30 μm. The PL spectra of the as-grown sample (shown at top) as well as the capped sample without patterning (shown in the middle) are also included for comparison. Of the two peaks, evidently the higher energy peak (at 1.08 eV) is from the area masked with SiO_2, while the lower energy peak (at 0.95 eV) is from the exposed window areas. The amounts of blue-shift in the peaks are 150 and 20 meV for the higher and lower energy peaks, respectively. The larger shift represents enhanced QW intermixing by the dielectric, while the smaller shift indicates only self-interdiffusion was effective in the window areas.

The PL spectra observed from the areas having different stripe widths are shown in Fig. 7(a) and (b). At 2 μm width, the PL signals corresponding to SiO_2 masked and exposed areas did not separate. The vacancies diffuse laterally as well as vertically and this lateral resolution made the two peaks merge into one broad spectrum. At the stripe width of 4 μm, the separation of the two peaks is not yet clear, but at 6 μm and larger, the two peaks are shown clearly separated. Thus we observe that amount of lateral diffusion is more than 2 μm, but less than 3 μm.

Since the technology described above allows lateral bandgap engineering without the expensive epitaxial regrowth, one can find many applications in fiber optic communications. The potential devices include all optical switches [21] and wavelength-division demultiplexers [22].

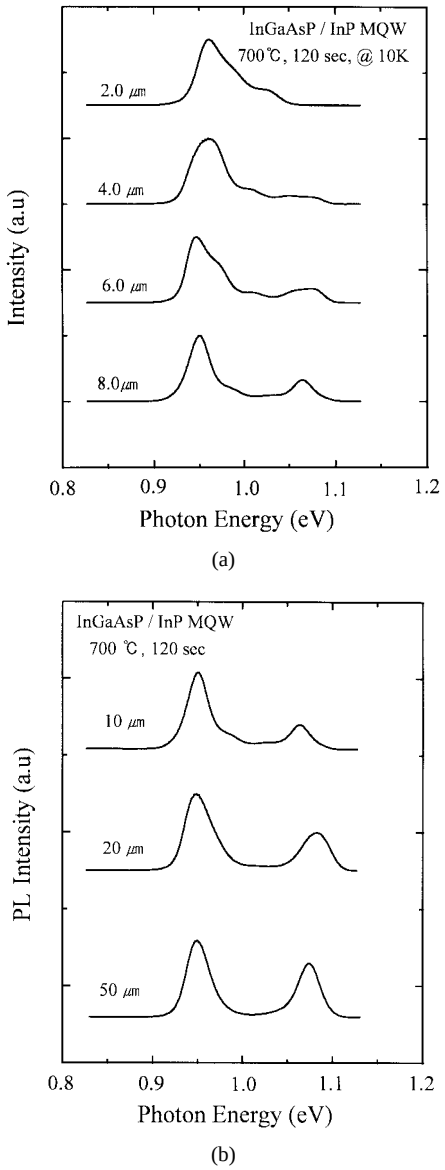

Fig. 7. Normalized PL spectra (at 10 K) after selective-area intermixing at various stripe width. The width of the window was set equal to the stripe width. (a) When stripe width ranged from 2 to 8 μm. (b) When stripe width ranged from 10 to 50 μm. The annealing was done at 700 °C for 120 s.

IV. Summary and Conclusion

We have investigated selective intermixing of InGaAsP–InP MQW structure by an IFVD method using SiO_2 capping and InGaAs cap layers. A substantial bandgap blue-shift, as large as 170 meV at 850 °C for 30 s, was obtained and the value of the shift was found controllable by changing anneal temperature and time. We explained through modeling that the diffusion coefficient for the group-V interdiffusion is slightly higher than, but comparable to that for the group-III. The corresponding coefficients for the group-III and -V interdiffusion were 1.6×10^{-16} cm^{-2}/s, 2×10^{-16} cm^{-2}/s, respectively at 700 °C. In the area-selectivity study, clearly separated PL signals, each representing intermixed and unintermixed areas, were observed from samples where striped oxide patterned were applied. The effective lateral diffusion at 700 °C were estimated 2.9 μm This technique enables creation of regions with largely different bandgaps within a chip, with simply use of patterned SiO_2 film, thus proving to be a very useful and low-cost technology for future optical device fabrication.

References

[1] J. H. Marsh, "Quantum well intermixing," *Semiconduct. Sci. Technol.*, vol. 8, pp. 1136–1155. 1993.
[2] M. Aoki, M. Suzuki, H. Sano, T. Kawano, T. Ido, T. Taniwatari, K. Uomi, and A. Takni, "InGaAs/InGaAsP MQW electroabsorption modulator integrated with a DFB laser fabricated by band-gap energy control selective-area MOCVD," *IEEE J. Quantum Electron.*, vol. 29, pp. 2088–2096, 1993.
[3] W. D. Laidig, N. Holonyak, Jr. M. D. Camras, K. Hess, J. J. Coleman, P. D. Dapkus, and J. Bardeen, "Disorder of an AlAs-GaAs superlattice by impurity diffusion," *Appl. Phys. Lett.*, vol. 38, pp. 776–778, 1981.
[4] S. A. Schwarz, P. Mei, T. Venkatesan, R. Bhat, D. M. Hwang, C. L. Schwartz, M. Koza, L. Nazar, and B. J. Skromme, "InGaAs/InP superlattice mixing induced by Zn or Si diffusion," *Appl. Phys. Lett.*, vol. 53, pp. 1051–1053, 1988.
[5] S. Charbonneau, P. L. Poole, P, G. Piva, G. C. Aers, E. S. Kotles, M. Fallahi, J.-J. He, J. P. Mccaffery, M. Buchanan, and M. Dion, R. D. Goldberg, and I. V. Mitchell, "Quantum-Well intermixing for optoelectronic integration using high energy ion implantation," *J. Appl. Phys.*, vol. 78, pp. 3697–3705, 1995.
[6] J. Z. Wan, D. A. Thompson, and J. G. Simmons, "Ion implantation induced compositional intermixing in the InGaAs/InP MQW system for wavelength shifted waveguides," *Nucl. Instrum. Meth. Phys., Res. B*, vol. 106, pp. 461–465, 1995.
[7] L. J. Guido, N. Holonak, Jr., K. C. Hsieh, R. W. Kaliski, W. E. Plano, R. D. Burnham, R. L. Thornton, J. E. Epler, and T. L. Paoli, "Effects of dielctric encapsulation and As overpressure on Al-Ga interdiffusion in $Al_xGa_{1-x}As$-GaAs quantum-well heterostructures," *J. Appl. Phys.*, vol. 61, pp. 1372–1379, 1987.
[8] I. Gontijo, T. Krauss, J. H. Marsh, and R. M. De La Rue, "Postgrowth control of GaAs/AlGaAs quantum well shapes by impurity-free vacancy diffusion," *IEEE. J. Quantum Electron.*, vol. 30, pp. 1189–1195, 1994.
[9] E. V. K. Rao, A. Hamoudi, Ph. Krauz, M. Juhel, and H. Thibierge, "New encapsulatn source for III–V quantum well disordering," *Appl. Phys. Lett.*, vol. 66, pp. 472–474, 1995.
[10] A. Pepin, C. Vieu, M. Schneider, and H. Launois, "Evidence of stress dependence in SiO_2/Si_3N_4 encapsulation-based layer disordering of GaAs/AlGaAs quantum well heterostructures," *J. Vac. Sci. Technol. B*, vol. 15, pp. 142–153, 1997.
[11] M. Katayama, Y. Tokuda, T. Y. Inoue, A. Usami, and T. Wada, "Ga out-diffusion in rapid-thermal-processed GaAs with SiO_2 encapsulants," *J. Appl. Phys.*, vol. 69, pp. 3541–3545, 1991.
[12] Y. Suzuki, H. Iwamura, T. Miyazawa, A. Wakatsuki, and O. Mikami, "Polarization-dependent refractive-index change induced by superlattice disordering," *IEEE J. Quantum Electron.*, vol. 32, pp. 1922–1931, 1996.
[13] J. H. Lee, S. K. Si, Y. B. Moon, E. J. Yoon, and S. J. Kim, "Bandgap tunning of $In_{0.53}Ga_{0.47}As$/InP multquantum well structure by impurity free vacancy diffusion using $In_{0.53}Ga_{0.47}As$ cap layer and SiO_2 dielectric capping," *Electron. Lett.*, vol. 33, pp. 1179–1180, 1997.
[14] A. McKee, C. J. McLean, G. Lullo, A. C. Bryce, M. De La Rue, J. H. Marsh, and C. C. Button, "Monolithic integration in InGaAs-InGaAsP multi-quantum well structures using laser intermixing," *IEEE J. Quantum Electron.*, vol. 33, pp. 45–55, 1997.
[15] S. J. Fancey, G. S. Buller, J. S. Massa, A. C. Walker, C. J. McLean, A. McKee, A. C. Bryce, J. H. Marsh, and R. M. De La Rue, "Time-resolved photoluminescence microscope of GaInAs/GaInAsP quantum wells intermixed using a pulsed laser technique," *J. Appl. Phys.*, vol. 79, pp. 9390–9392, 1996.
[16] A. Hamoudi, E. V. K. Rao, Ph. Krauz, A. Ramadane, A. Ougazzaden, D. Robein, and H. Thibierge, "Controlled disordering of compressively strained InGaAsP multiple quantum wells under SiO:P encapsulant and application to laser-modulator integration," *J. Appl. Phys.*, vol. 78, p. 5638, 1995.
[17] J. Micallef, E. H. Li, and B. L. Weiss, "Effects of interdiffusion on the sub-band-edge structure of $In_{0.53}Ga_{0.47}As$/InP single quantum wells," *J. Appl. Phys.*, vol. 73, p. 7625, 1993.
[18] J. Singh, *Semiconductor Optoelectronics Physics and Technology*, S. W. Director, Ed. New York: McGraw-Hill, p. 90.

[19] P. K. Bhattacharya, M. V. Rao, and M-J. Tsai, "Growth and photoluminescence spectra of high-purity liquid phase epitaxial $In_{0.53}Ga_{0.47}As$," *J. Appl. Phys.*, vol. 54, pp. 5096–5102, 1983.
[20] A. Hamoudi, A. Ougazzaden, P. Krauz, K. Rao, M. Jubel, and H. Thibierge, "An optical study of interdiffusion in strained InP-based heterostructures," *Jpn. J. Appl. Phys.*, vol. 34, pp. 36–41, 1995.
[21] S. Shi, P. Li Kam Wa, A. Miller, J. Pamulapati, P. Cooke, and M. Dutta, "Multi-quantum well zero gap directional coupler with disordered branching waveguides," *Appl. Phys. Lett.*, vol. 66, pp. 79–81, 1995.
[22] A. N. M. Masum Choudhury, P. Melman, A. Silletti, E. S. Koteles, B. Foley, and B. Elman, "Metal-semiconductor-metal demultiplexing waveguide photodetectors in InGaAs/GaAs quantum well structures by selective bandgap tuning," *IEEE Photon. Technol. Lett.*, vol. 3, pp. 817–819, 1991.

Sang Kee Si, photograph and biography not available at the time of publication.

Deok Ho Yeo, photograph and biography not available at the time of publication.

Kyung Hun Yoon, photograph and biography not available at the time of publication.

Sung June Kim, photograph and biography not available at the time of publication.